58930-00-105

ANL/CP--72496

DE91 011120

ENHANCED FLUX PINNING BY CRYSTAL DEFECTS IN MELT-TEXTURED $YBa_2Cu_3O_x$

Donglu Shi[1], K.C. Goretta[2], J. G. Chen[3], and S. Salem-Sugui, Jr.[1]

[1]Materials Science Division
[2]Materials and Components Technology Division
Argonne National Laboratory, Argonne, IL 60439
[3]Department of Materials Science and Engineering
University of Illinois at Urbana, Urbana, IL 61801

PRESENTED AT: TMS Annual Meeting in New Orleans, LA, 2/17-21/91

*Work supported by U.S. Department of Energy, BES-Materials Sciences under contract #W-31-109-ENG-38.

Enhanced Flux Pinning by Crystal Defects in Melt-Textured $YBa_2Cu_3O_x$*

Donglu Shi, K. C. Goretta,[1] J. G. Chen,[2] and S. Salem-Sugui, Jr.
Materials Science Division
[1]Materials and Components Technology Division
Argonne National Laboratory
Argonne, IL 60439

Invited talk to be presented at the TMS Annual Meeting in New Orleans, Louisiana, February 17–21, 1991.

PACS # 74.40+k, 74.60.Ge, 74.30.Ci

---

* Work supported by the U. S. Department of Energy, BES – Materials Science, under Contract W-31-109-ENG-38.

2 Also with the Department of Materials Science and Engineering, University of Illinois at Urbana, Urbana, IL 61801

ENHANCED FLUX PINNING BY CRYSTAL DEFECTS IN MELT–TEXTURED $YBa_2Cu_3O_x$

Donglu Shi, K. C. Goretta, J. G. Chen, and S. Salem–Sugui, Jr.

Argonne National Laboratory
Argonne, IL 60439

Abstract

$YBa_2Cu_3O_x$ bars have been partially melted to develop highly textured microstructures. Transmission electron microscopy (TEM) revealed the presence of a large amount of intragranular defects such as dislocations and stacking faults, and a few Y_2BaCuO_5 particles, within the matrices. These crystal defects strongly affected intragranular J_c values and the flux–creep behavior. After annealing the textured samples at high temperature for 80 h, considerable reduction in the magnetization J_c was observed. This microstructure–related J_c variation indicated that the lattice defects observed by TEM were connected with the observed enhanced flux pinning. Possible pinning mechanisms are discussed.

Introduction

Critical current densities and flux pinning have been the most important issues in superconductivity from both basic research and practical application points of view. In particular, flux pinning mechanisms in high–T_c superconductors have generated great interest among solid–state physicists and materials scientists. An extensively studied problem has been identification of the flux–pinning centers in high–T_c superconductors. It has been proposed that the strong pinning effects in $YBa_2Cu_3O_x$ (123) are associated with the oxygen deficiency (1). Other studies showed that twin boundaries in 123 can also cause pinning, but that the pinning strength is rather weak (2–4). Although some experimental results on melt–textured 123 have shown increased flux–pinning effects, there have been no conclusive data indicating the specific crystal defects that are responsible for strong flux pinning (4–8).

In this paper, we present experimental data on flux pinning and magnetic relaxation in melt–textured, grain–oriented bulk 123 samples. We show close correlations between critical currents and microstructural defects in the melt–textured samples. We also discuss the possible pinning mechanisms associated with the crystal defects, such as edge dislocations and stacking faults, observed in transmission electron microscopy (TEM).

Experimental Methods

All specimens were prepared from 123 powder synthesized by solid–state reaction of Y_2O_3, $BaCO_3$, and CuO. Well–mixed powders were calcined for 4 h at 800°C in flowing oxygen at a reduced pressure of about 2.6×10^2 Pa. The resultant powder was phase–pure by X–ray diffraction and differential thermal analysis (9). Five–g bars were cold–pressed at 80 MPa in a 50–mm by 7.6–mm hardened steel die. The bars were placed on Al_2O_3 plates and sintered for 3 h at 985°C in flowing oxygen. The sintered bars were melt–textured in air in a vertical tube furnace. The texturing heat treatment consisted of: rapid insertion into a furnace at 1150°C, a hold for 0.2 h, cooling in 0.1 h to 1050°C, followed by cooling to 950°C at 1°C/h. Subsequent annealing in pure oxygen at 450°C increased the oxygen content to the desired level. Detailed information about the melt–texturing can be found in Ref. 10.

Small portions from one melt–textured specmen and one sintered specimen were crushed seperately in an agate mortar and pestle so that intragranular J_c values could be measured. The specimens were first cooled in liquid nitrogen to promote fracture and minimize formation of dislocations during crushing. Half of the powder from the crushed melt–textured sample was annealed in air for 80 h at 880°C in an attempt to remove dislocations and stacking faults. The other half was given only the lower temperature oxygenation anneal. For all powders, the final anneal was at 450°C in oxygen for 4 h. The powder particle sizes were all about 5–10 μm and were measured from scanning electron microscopy (SEM) photographs.

The magnetic hysteresis and relaxation data were taken with a commercial superconducting quantum interference device (SQUID) at various temperatures and fields up to 5 T. The magnetic relaxation data were obtained by the zero–field–cooled method: the sample was first cooled to a temperature below T_c in zero field and a magnetic field was then established to a given value; for each test, the first data point was taken 180 s after the field stabilized. The TEM was performed on a Philips 420 electron microscope.

Results and Discussion

Figure 1 shows the typical microstructure of a melt-textured sample. As revealed by SEM, a well-textured, uniform microstructure extends through the entire sample. Careful SEM study has shown that the sample is extremely dense and is nearly free of voids. More importantly, only small concentrations of Y_2BaCuO_x (211) are found in the melt-textured samples. High concentrations of edge dislocations with Burgers vectors of [100] or [010] were observed by TEM (10,11). The dislocation density has been estimated to be $10^{10}/cm^2$. Most of the dislocations are located in the a–b plane, which may be the easy-slip plane for 123 structure. A considerable amount of partial dislocations were also observed (indicated by the arrows in Fig. 2).

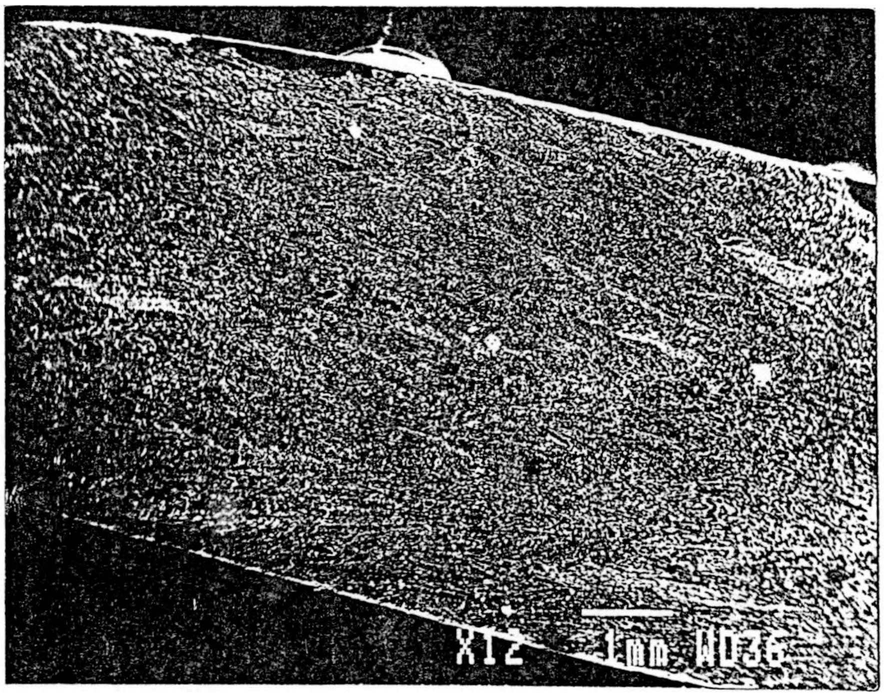

Figure 1 – SEM micrographs of melt-textured specimen.

Figure 3 shows the magnetization J_c versus applied field at various temperatures for samples with different microstructures obtained by melt-texturing, melt-texturing and high-temperature annealing, and conventional sintering. The magnetization J_c values were calculated from the Bean critical-state model (12): $J_c = 30\ \Delta M/d$, where ΔM is the magnetic hysteresis difference and d is the particle size. For comparison, the J_c of an as-sintered bulk sample was included. It is emphasized that these samples were all in powder form, that the powders had roughly comparable average particle sizes, and that all of the samples received identical oxygenation treatments. It should also be noted that annealing did not affect the particle sizes of the samples.

As shown in Fig. 3, up to 5 T, the melt-textured sample had the highest J_c at 10 K and 30 K. However, after an identical sample was annealed at 880°C for 80 h, the J_c was considerably reduced, especially at fields below 3 T. At 10 K and 2 T, for example, after annealing, the J_c of the melt-textured sample decreased from 1.5×10^7 A/cm^2 to 5×10^6 A/cm^2. For the same conditions, the J_c of the as-sintered sample was about 8×10^5 A/cm^2. The reduction in J_c with annealing becomes smaller at higher field. At 30 K, only a small variation in J_c due to the annealing treatment is observed above 3.5 T.

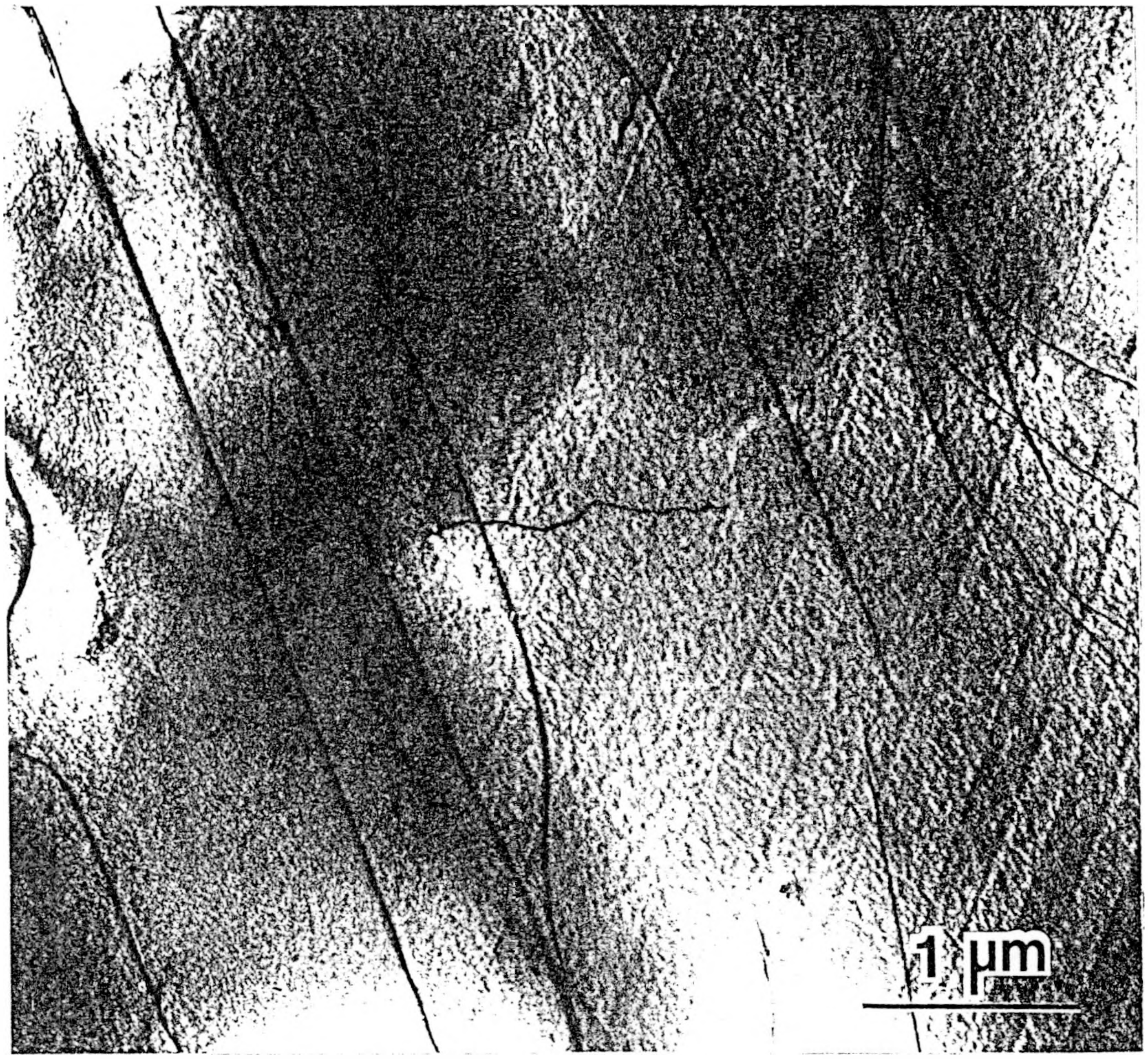

Figure 2 – TEM of edge dislocations and partial dislocations in a melt–textured specimen.

The effect of annealing becomes more pronounced as the testing temperature is increased to 50 K and 77 K. As can be seen in Fig. 3c, a much greater reduction in J_c over the entire field region is observed at 50 K. However, the overall field dependencies of J_c at 50 K are similar to those at 10 K and 30 K. At 77 K, the melt–textured sample has a J_c value of about 1 x 10^5 A/cm^2 at 2 T, which agrees well with previously reported data (13,14). At 77 K, the J_c dropped drastically after the melt–textured sample was annealed at high temperature (Fig. 3d). The field dependence of J_c for the annealed sample (MT–annealed) was comparable to that of the as–sintered sample. At 2 T, J_c falls to about 2 x 10^3 A/cm^2. In Fig. 4, we plot J_c versus temperature at 1 T for all of the samples shown in Fig. 3. We found that critical current density follows the relation $J_c \sim \exp(T/T_c)$. This is different from most previous studies, in which a power–law decay has been observed. However, we were unable to fit the temperature dependence of J_c in the as-sintered samples with an exponential function. The exponential temperature dependencies of J_c in the melt-textured samples (annealed and as–textured) indicate a common pinning mechanism associated with the unique microstructure of these materials.

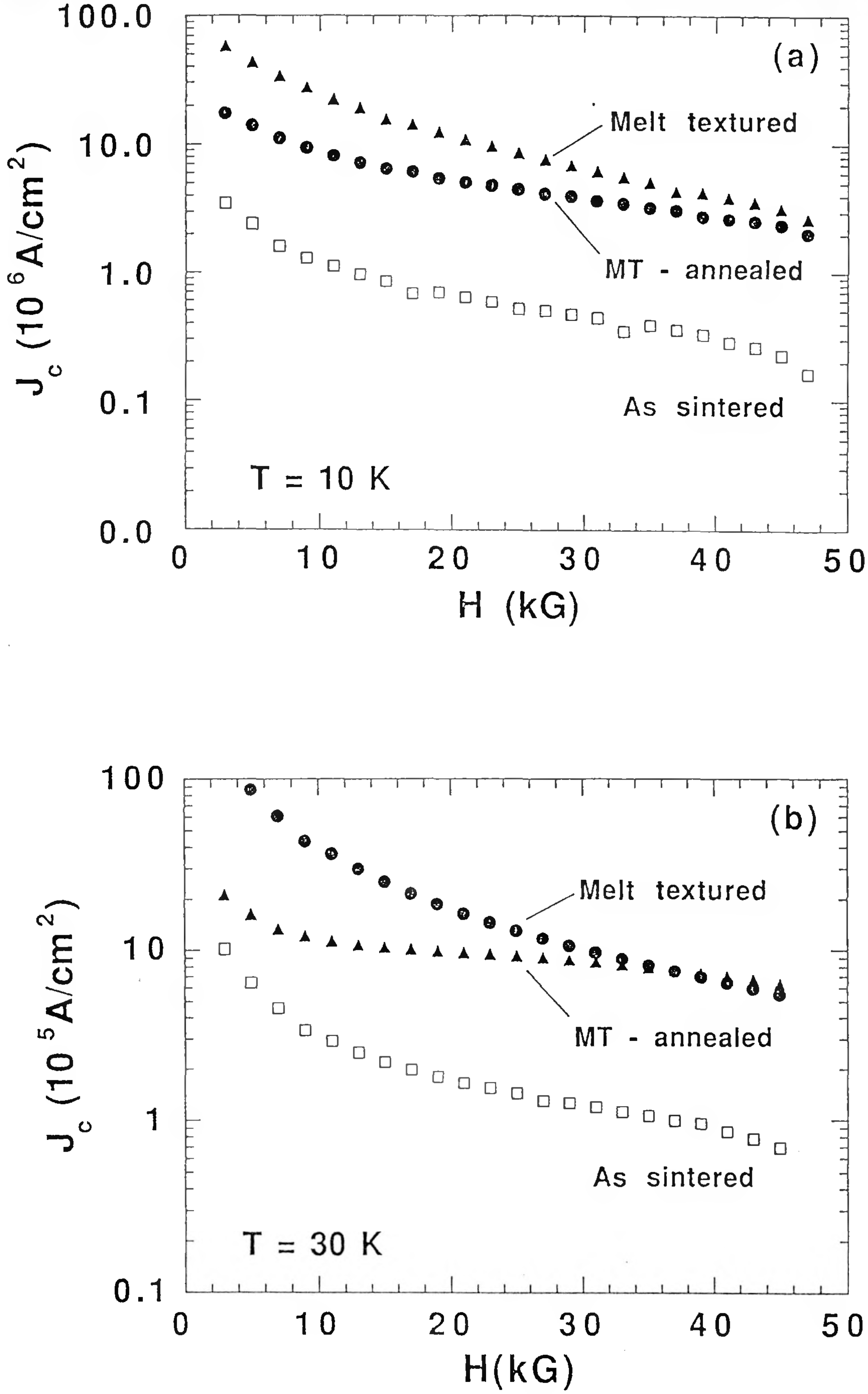

Figure 3 – J_c versus applied field for the various samples indicated at: (a) 10 K and (b) 30 K.

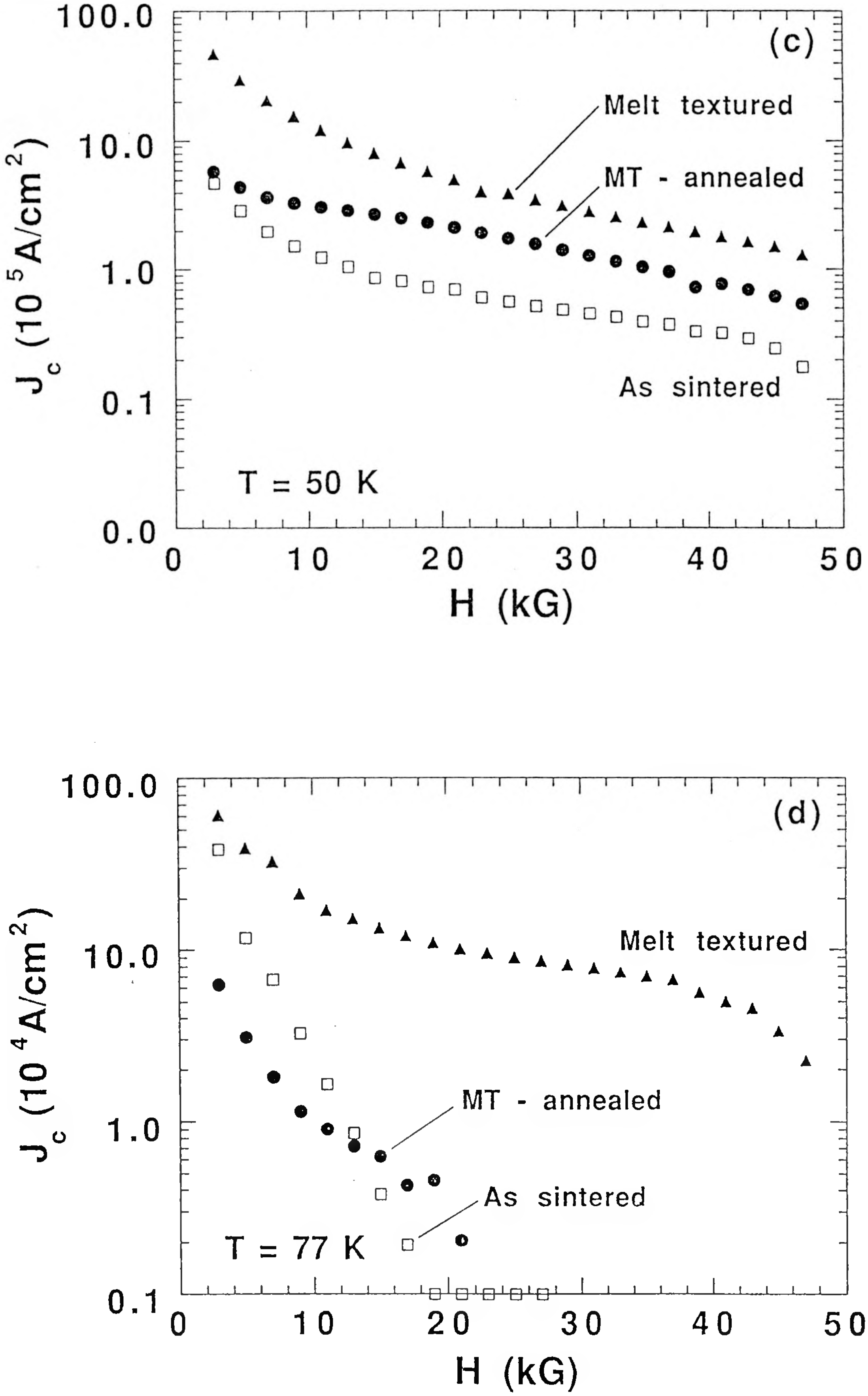

Figure 3 – J_c versus applied field for the various samples indicated at: (c) 50 K and (d) 77 K.

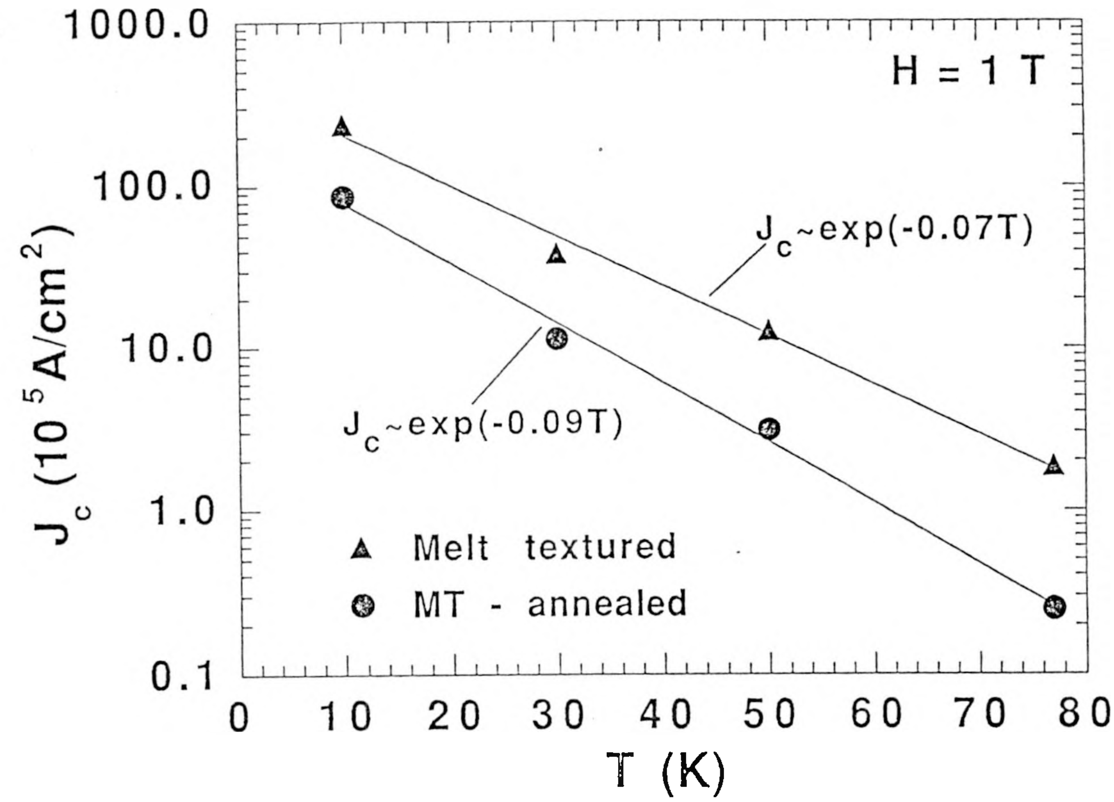

Figure 4 – J_c versus temperature at 1 T for the melt–textured samples; the solid lines have been fit to the formula shown.

The J_c in melt–textured 123 is of great interest. As mentioned previously, the most commonly observed crystal defects in 123 are (110) twin boundaries. These boundaries have similar characteristics in both as–sintered and melt–textured samples: the twin spacing is approximately the same, d ≈ 1300–1500 Å. The pinning mechanisms of twin boundaries have been studied by both inductive and transport experiments (2-4). The contribution of twin boundary pinning has been found to be small and is on the same order of magnitude for both melt–textured and as–sintered samples. However, due to the partial melting, much greater crystal inhomogeneity was detected in the melt–textured samples. From TEM, we have found that the partially melted materials possess higher densities of dislocations than do the as–sintered samples. High–resolution TEM results have shown that the dimensions of these dislocations and stacking faults are comparable to the lattice atomic scale, which is on the order of the coherence length of 123. It is, therefore, reasonable to assume them to be appropriate pinning centers. In addition, some 211 precipitates are always found within the matrices of melt–textured materials (4-8,10). We have found that a strain field is present at the interfaces between 123 and 211 because of the lattice and thermal expansion mismatches between the two phases. The pinning from 211 precipitates will be discussed later.

Some dislocations are annihilated by annealing at elevated temperatures. Thermal activation can induce dislocations to glide and to climb. Glide occurs along the slip plane and requires the presence of a shear stress. Climb involves diffusion of point defects and results in motion perpendicular to the slip plane. For both glide and climb, dislocations of opposite sign are drawn toward each other because of their stress fields. They meet and annihilate by reforming a region of undislocated lattice. Annihilation of partial dislocations also eliminates their attendant stacking faults.

The 211 phase cannot be removed by high–temperature annealing. But, the strain field at the interfaces may be relaxed to a certain extent. Although it has been claimed that the 211 precipitates can act as strong flux pinning centers (15), our results indicate that for our melt–textured samples, dislocations and stacking faults are more likely to be the effective flux pinners. Figure 3 clearly shows the J_c reduction due to the high–temperature annealing process, and our SEM observations indicate that there was no change in the 211 phase because of annealing. Further, oxygen inhomogeneity should not play an important role in these results because finely powdered samples are easily oxygenated.

Conclusion

Melt–textured 123 bars with high intragranular J_c values were produced. High–temperature annealing reduced the J_c values. Large amounts of dislocations and stacking faults were observed by TEM. These crystal defects were shown to be effective flux pinning centers. J_c values dropped as the concentrations of these defects decreased.

Acknowledgments

This work was supported by the U. S. Department of Energy, Basic Energy Sciences–Materials Sciences, under Contract W–31–109–ENG–38. J.G.C. is also with the Department of Materials Science and Engineering, the University of Illinois at Urbana, Urbana, IL 61801. The 123 powder was provided by our colleagues U. Balachandran and M. T. Lanagan and some of the bars were made by A. C. Biondo.

References

1. D. Shi and M. S. Boley, Supercond. Sci. Technol., 3 (1990), 285–288.

2. G. T. Dolan, G. V. Chandrashekhar, T. R. Dinger, C. Field, and F. Holzber, Phys. Rev. Lett., 62 (1989), 827–829.

3. D. Shi, M. Xu, M. S. Boley, and U. Welp, Physica C, 160 (1989), 417–423.

4. M. Murakami, M. Morita, and N. Koyama, Jpn. J. Appl. Phys., 28 (1989), L1754–L1756.

5. S. Jin, T. H. Tiefel, R. C. Sherwood, M. E. Davis, R. B. van Dover, G. W. Kammlott, R. A. Fastnacht, and H. D. Keith, Appl. Phys. Lett., 52 (1988), 2074–2076.

6. K. Salama, V. Selvamanickam, L. Gao, and K. Sun, Appl. Phys. Lett., 54 (1989), 2352–2354.

7. M. Murakami, M. Morita, K. Doi, and K. Miyamoto, Jpn. J. Appl. Phys., 28 (1989), 1189–1194.

8. P. J. McGinn, W, Chen, N. Zhu, U. Balachandran, and M. T. Lanagan, Physica C, 165 (1990), 480–484.

9. U. Balachandran, R. B. Poeppel, J. E. Emerson, S. A. Johnson, M. T. Lanagan, G. A. Youngdahl, D. Shi, K. C. Goretta, and N.G. Eror, Mater. Lett., 8 (1989), 454–456.

10. D. Shi, M. M. Fang, J. Akujieze, M. Xu, J. G. Chen, and C. Segre, Appl. Phys. Lett., 57 (1990), 2606–2608.

11. D. Shi, K. C. Goretta, J. G. Chen, and A. C. Biondo, (Paper presented at the 2nd International Ceramic Science and Technology Congress, Orlando, Florida, 14 November 1990).

12. C. P. Bean, Phys. Rev. Lett., 8 (1962), 250–253.

13. D. Shi, H. Krishnan, J. M. Hong, D. Miller, P. J. McGinn, W. H. Chen, M. Xu, J. G. Chen, M. M. Fang, U. Welp, M. T. Lanagan, K. C. Goretta, J. T. Dusek, J. J. Picciolo, and U. Balachandran, J. Appl. Phys., 68 (1990), 228–232.

14. P. J. McGinn, M. Black, and A. Valenzuela, Physica C, 156 (1988), 57–61.

15. K. Yamaguchi, M. Murakami, H. Fujimoto, S. Gotoh, N. Koshizuka, and S. Tanaka, Jpn. J. Appl. Phys., 29 (1990), L1428–L1431.